



HAL
open science

On the morphological stability of multicellular tumour spheroids growing in porous media

Chiara Giverso, Pasquale Ciarletta

► To cite this version:

Chiara Giverso, Pasquale Ciarletta. On the morphological stability of multicellular tumour spheroids growing in porous media. *European Physical Journal E: Soft matter and biological physics*, 2016, 39 (10), pp.92. 10.1140/epje/i2016-16092-7 . hal-01383173

HAL Id: hal-01383173

<https://hal.sorbonne-universite.fr/hal-01383173>

Submitted on 18 Oct 2016

HAL is a multi-disciplinary open access archive for the deposit and dissemination of scientific research documents, whether they are published or not. The documents may come from teaching and research institutions in France or abroad, or from public or private research centers.

L'archive ouverte pluridisciplinaire **HAL**, est destinée au dépôt et à la diffusion de documents scientifiques de niveau recherche, publiés ou non, émanant des établissements d'enseignement et de recherche français ou étrangers, des laboratoires publics ou privés.

On the morphological stability of multicellular tumour spheroids growing in porous media

Chiara Giverso¹ and Pasquale Ciarletta^{1,2a}

¹ Dipartimento di Matematica - MOX, Politecnico di Milano, Piazza Leonardo da Vinci, 32 - 20133 Milano, Italy;

² CNRS and Sorbonne Universités, UPMC Univ Paris 06, UMR 7190, Institut Jean le Rond d'Alembert, 4 place Jussieu case 162, 75005 Paris, France

Received: date / Revised version: date

Abstract Multicellular tumour spheroids (MCTSs) are extensively used as *in-vitro* system models for investigating the avascular growth phase of solid tumours. In this work, we propose a continuous growth model of heterogeneous MCTSs within a porous material, taking into account a diffusing nutrient from the surrounding material directing both the proliferation rate and the mobility of tumour cells. At the time scale of interest, the MCTS behaves as an incompressible viscous fluid expanding inside a porous medium. The cell motion and proliferation rate are modelled using a non-convective chemotactic mass flux, driving the cell expansion in the direction of the external nutrients' source. At the early stages, the growth dynamics is derived by solving the quasi-stationary problem, obtaining an initial exponential growth followed by an almost linear regime, in accordance with experimental observations. We also perform a linear-stability analysis of the quasi-static solution in order to investigate the morphological stability of the radially symmetric growth pattern. We show that mechano-biological cues, as well as geometric effects related to the size of the MCTS subdomains with respect to the diffusion length of the nutrient, can drive a morphological transition to fingered structures, thus triggering the formation of complex shapes that might promote tumour invasiveness. The results also point out the formation of a retrograde flow in the MCTS close to the regions where protrusions form, that could describe the initial dynamics of metastasis detachment from the *in-vivo* tumour mass. In conclusion, the results of the proposed model demonstrate that the integration of mathematical tools in biological research could be crucial for better understanding the tumour's ability to invade its host environment.

PACS. 87.18.Hf Spatiotemporal pattern formation in cellular populations – 87.18.Gh Cell-cell communication; collective behavior of motile cells – 46.32.+x Static buckling and instability

1 Introduction

A multicellular tumour spheroid (MCTS) is an ensemble of tumour cells organized in a multi-layered structure^{1,2}. In general, a MCTS consists of a central core of necrotic cells, surrounded by a layer of quiescent (*i.e.* dormant) cells and an outer rim of proliferating cells¹⁻⁴. MCTSs are widely used *in vitro* to study the early stages of avascular tumour growth and to assess the efficacy of anti-cancer drugs and therapies, since their growth and structure resemble the *in vivo* avascular phase of solid tumour invasion. Such an early growth phase is characterized by diffusion-limited growth, since the tumour absorbs vital nutrients via diffusion from the external environment^{1,3,5}. Thus, diffusion may become suddenly ineffective in the center of the tumour mass, forming a characteristic necrotic core (see Fig. 1-a). At later stages, a solid tumour is characterized by the occurrence of angiogenesis

(*i.e.* the process by which the tumour induces new blood vessels formation from the nearby existing vasculature), thus switching to a vascular growth phase^{6,7}.

The analysis of the avascular growth phase in tumours has attracted a lot of interest in the mathematical and physical research communities, and a large number of *in silico* mathematical models has been proposed^{2,8-16}. Thanks to the controllability and the reproducibility of the experimental setting, MCTS has become a widely used system model for the development of theoretical models.

The classical approach of deterministic tumour model comprised an ordinary differential equation (ODE), derived from either mass conservation or population dynamics, coupled with at least one reaction-diffusion equation, representing the spatio-temporal distribution of vital nutrients or chemical signals inside the tumour^{2,9-12,14,15,17}. Only recently, many authors have extended such models including the pivotal role of mechanics in tumour growth. In most cases, fluid-like constitutive equations have been used to model the tumour mass¹⁸⁻²⁶. This choice is obvi-

^a *e-mail*: pasquale.ciarletta@polimi.it

ously only an approximation of the by far more complex behaviour of cellular aggregates, that also display solid-like properties related to the adhesive characteristics of cells²⁷ and to the mechanical properties of the single cell in the cluster. Thus, in some limiting cases, cell aggregates are better described as solids with linear or eventually nonlinear elasticity, in which compressive and shear loads are balanced by the solid stress in the body, depending on the strain of its material points^{28–33}. A solid-like constitutive equation has been advocated for its suitability of accounting for both residual stresses^{29,32,34} and the plastic behaviour of cellular aggregates^{35–37}. Even though these considerations support the idea that a cellular aggregate can behave as a solid at some extent, experimental evidences^{26,38,39} have shown that aggregates behave as elastic solids on short timescales (of the order of a few minutes) but display a fluid-like behaviour at longer times. Furthermore, it was shown that cellular aggregates behave as an elastic solids at time scales short compared to that of cell division and apoptosis, and as a fluid (with the traceless stress that relaxes to zero) for long times⁴⁰. Thus the description of MCTSs as a liquid is widespread.

Even though the existing mathematical models on both solid tumours and MCTSs successfully reproduce the experimentally observed growth dynamics^{2,9–12,14,15,17,41,42}, they poorly consider the mechanical and chemical interaction with the surrounding environment. Furthermore, most approaches assume that the initial spherical symmetry is preserved during the growth of the aggregate^{28–30}, whilst only in few cases^{11,12,15} the development of tumour irregular contours has been taken into account. Indeed, it is known that some solid tumours, *e.g.* carcinomas, grow almost spherically only in the first stages of their progression^{1,3,5}, while they might show a less defined and even asymmetric outer boundary⁴³ (see Fig. 1-b). Since higher irregular contours usually indicate aggressive tumours, the capability to undergo a morphological transition might promote tumour infiltration and invasion within the surrounding tissue^{2,11,12,15,44–46}. Thus, it has been proposed that some measure of the irregularity of a tumour boundary (*e.g.* its fractal index measured via particular medical imaging techniques such as computerized tomography scans), may provide clinicians with useful information for its prognosis and treatment^{44–46}, being potentially useful in predicting the efficacy of drug treatment or chemotherapy^{47,48}.

In this work we go beyond the state-of-the art in the field^{2,49,50} by proposing a mathematical model that accounts for the presence of a surrounding porous media with a finite thickness. Thus, nutrient diffusion from the external environment creates a chemical gradient that directs both the proliferation rate and the motility of the tumour cells. MCTS is modelled as a viscous fluid with adhesive interactions at the border, expanding inside a porous material.

This work is organized as follows. First, we introduce in Section 2 the mathematical model describing the expansion of an initially spherical tumour. In Section 3, we derive the radially-symmetric solution of the quasi-stationary

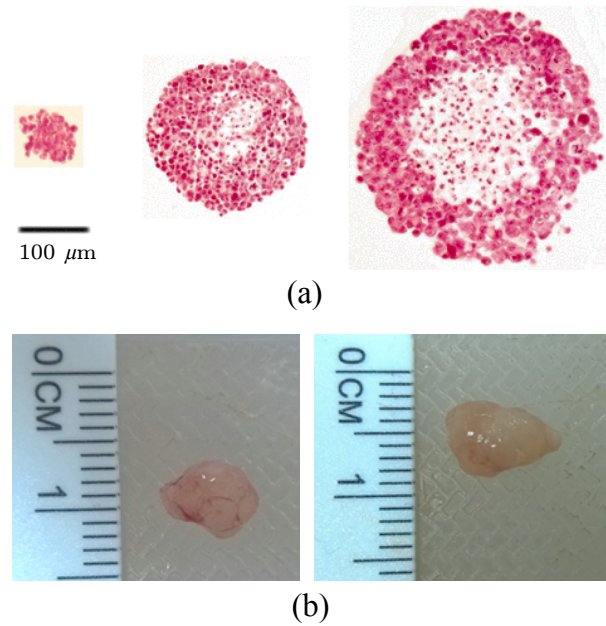


Figure 1. (a) Morphological evolution of a multicellular tumour spheroid of HeLa cells, showing the development of an undulated contour and a necrotic core (reproduced with permission from⁵¹). HeLa cells were trypsinized, counted and grown as multicellular spheroids using the liquid overlay technique. The sections were counterstained with hematoxylin and eosin to visualize the cytoplasm of the cells. The multicellular spheroid section is reproduced at days 0, 4 and 12, from left to right. (b) Solid tumours extracted from mice after orthotopic implant of MCF10CA1a cell lines in the mammary fat pad of the nude mice (courtesy of T. Stylianopoulos, Cancer Biophysics Laboratory, University of Cyprus).

problem. Then, we perform a linear stability on the quasi-static tumour growth. Finally, in Section 4, we discuss the modelling results with respect to the key chemo-mechanical and geometric parameters that govern the mathematical problems, highlighting the key mechano-biology effects that promote a morphological transition during tumour invasion.

2 Mathematical Model

The MCTS is modelled as a three dimensional continuum growing inside a rigid porous structure, representing the surrounding environment, usually extracellular matrix (ECM) or matrigel. In this respect, the proposed model refers to the *in vitro* case in which MCTS grows inside a three dimensional either natural medium (*e.g.* agarose gel, hyaluronic acid gel) or synthetic matrices scaffolds (*e.g.* polylactide and polyglycolide biodegradable structures mimicking a tissue-like environment)⁵².

The outer boundary of the tumour is considered as a freely moving material interface separating the tumour cells from the surrounding medium.

117 In particular, we account for the presence of a central re-
 118 gion of necrotic cells, surrounded by a layer of quiescent
 119 and proliferating cells. Thus, the whole domain Ω is di-
 120 vided in different regions, depending on the residing cel-
 121 lular population (see Fig. 2):

- the necrotic cells are located in the central core of the spheroid, in a region called $\Omega_N(t)$, with

$$\Omega_N(t) = \{(r, \theta) : r < R_N(t), 0 < \varphi \leq \pi, 0 < \theta \leq 2\pi\},$$

122 where R_N is the radius of the necrotic core, that might
 123 evolve in time;

- the proliferative and quiescent tumour cells are located in the region

$$\Omega_T(t) = \{(r, \theta) : R_N(t) < r < R_T(t), 0 < \varphi \leq \pi, 0 < \theta \leq 2\pi\},$$

124 where R_T is the radius of the spheroid, whose evolution
 125 in time represents the growth of the MCTS;

- the healthy space, composed by either the in vitro scaffold or the extracellular matrix, the extracellular liquid and possibly healthy cells (in vivo),

$$\Omega_H(t) = \{(r, \theta) : R_T(t) < r < R_{out}, 0 < \varphi \leq \pi, 0 < \theta \leq 2\pi\},$$

126 being R_{out} the outer boundary of the whole domain.

127 The boundary between the necrotic core and the prolifer-
 128 ative region is called $\partial\Omega_N(t)$, whereas the moving inter-
 129 face between the tumour region and the healthy space
 130 is denoted with $\partial\Omega_T(t)$. In the following we will con-
 131 sider that the interior boundary between the necrotic core
 132 and the quiescent-proliferative region does not evolve in
 133 time, since we are interested only in the evolution of the
 134 MCTS boundary, which is related to tumour infiltration
 135 inside the healthy region. Furthermore, we assume that
 136 the porous material is homogeneously distributed in the
 137 whole region $\Omega = \Omega_N \cup \Omega_T(t) \cup \Omega_H(t)$ and it is neither
 138 produced/degraded (*i.e.* behaves as inert matter), nor de-
 139 formed (*i.e.* structurally rigid) by the moving tumour cells.
 140 We will consider a single nutrient species (*e.g.* oxygen)
 141 with volume concentration $n(\mathbf{x}, t)$, diffusing from the fixed
 142 outer boundary $\partial\Omega$ through the porous material. Thus,
 143 we assume that the vascular network providing the source
 144 of nutrients is outside the modelled domain, and can be
 145 represented by a boundary term at $\partial\Omega$. The diffusion coef-
 146 ficient is a constant value D_n everywhere, but the nutrient
 147 is only consumed, with an uptake rate γ_n , in the region oc-
 148 cupied by the proliferative and quiescent cells. Indeed we
 149 consider that the consumption of nutrients in the healthy
 150 region is negligible. This is certainly the case of MCTS
 151 growing inside artificial/natural scaffolds, but, in a first
 152 approximation, it can be used also to model the in vivo
 153 condition^{20,53}, since the net consumption of nutrients in
 154 the extracellular healthy space is negligible compared to
 155 the uptake by tumor cells⁵⁴.

156 Thus, the 3D homogenized concentration per unit volume
 157 of this generic chemical species, indicated with $n(\mathbf{x}, t)$,
 158 obeys the following reaction-diffusion equation

$$\dot{n}(\mathbf{x}, t) = \begin{cases} D_n \nabla^2 n(\mathbf{x}, t) & \text{in } \Omega_N, \\ D_n \nabla^2 n(\mathbf{x}, t) - \gamma_n n(\mathbf{x}, t) & \text{in } \Omega_T(t), \\ D_n \nabla^2 n(\mathbf{x}, t) & \text{in } \Omega_H(t). \end{cases} \quad (1)$$

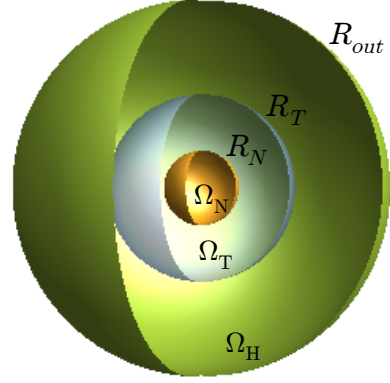


Figure 2. Representation of the domain used for the analytical analysis. At time $t = 0$, the three domains Ω_N , Ω_T and Ω_H are concentric spherical shells, with radius R_N , R_T and R_{out} , respectively. In this work, we consider that only the tumour boundary $\partial\Omega_T$ evolves in time.

159 We remark that, in principle, the uptake rate γ_n should
 160 depend on the tumour cell density, although, in the follow-
 161 ing, it will be considered homogeneous and constant over
 162 time. Even the diffusion coefficient D_n can be affected by
 163 the cell packing inside the tumor and by the extracellular
 164 matrix alignment and distribution. However, coherently
 165 with the hypothesis of an inert, rigid and homogeneous
 166 extracellular matrix distributed in the whole domain, the
 167 diffusion of nutrients can be assumed to be constant^{53,55}.
 168 The diffusing nutrient notably not only affects the growth
 169 of single individuals in the tumour but also directs cell
 170 movements, *e.g.* through chemotaxis^{56,57}. Therefore, we
 171 consider a non-convective mass flux term, \mathbf{m} , taking into
 172 account both tumour proliferation and chemotactic mo-
 173 tion, differently from the standard volumetric production
 174 rate considered in literature^{2,11–15}. Accordingly, the mass
 175 balance inside $\Omega_T(t)$ reads

$$\frac{d\rho}{dt} + \rho \nabla \cdot \mathbf{v} = \nabla \cdot \mathbf{m} \quad \text{in } \Omega_T(t). \quad (2)$$

176 where ρ is the tumour cell density, which is approximately
 177 the same of water. Since mass transport phenomena in
 178 MCTSs are driven by the local concentration of chemicals,
 179 the mass flux vector appearing in Eq. (2) should depend
 180 on nutrient availability. A simple constitutive law for \mathbf{m}
 181 can be taken in the form of a chemotactic term^{56,58}, *i.e.*
 182 $\mathbf{m} = \chi \rho \nabla n$, where χ is the chemotactic coefficient, here
 183 considered constant. Consequently, the mass flux \mathbf{m} de-
 184 scribes the expansion of the tumour due to proliferation
 185 and driven by chemotaxis towards higher concentration of
 186 nutrients.

187 Assuming that the living aggregate can be macroscopically
 188 modelled as a Newtonian fluid, Darcy's law describes its
 189 motion inside the inert, porous surrounding medium^{2,18}.
 190 Thus, the cell velocity \mathbf{v} is related to the pressure field p

through

$$\mathbf{v} = -K_p \nabla p, \quad (3)$$

where K_p is related to the permeability of the medium, k , and the viscosity of the cellular material, μ , by $K_p = k/\mu$. Assuming the incompressibility of the cellular spheroid, which is mostly composed by water, we impose $d\rho/dt = 0$ in Eq. (2), so that the relation between the pressure p and the nutrient concentration n reads

$$\nabla^2 p = -\frac{\chi}{K_p} \nabla^2 n \quad \text{in } \Omega_T(t), \quad (4)$$

which has been obtained substituting the Darcy's law (3) and the constitutive relations for \mathbf{m} in the mass balance equation (2). In summary, the coupling of Eq. (1) with Eq.(4), complemented by a proper set of boundary conditions (BCs), describes the macroscopic evolution of the avascular tumour inside the healthy tissue.

In particular, for the pressure we impose the Young-Laplace equation at the moving boundary $\partial\Omega_T(t)$ and the null velocity of the tumour cells at the fixed boundary $\partial\Omega_N$, *i.e.*

$$p = p_0 - \sigma_b C \quad \text{on } \partial\Omega_T(t), \quad (5)$$

$$\mathbf{v}_{\partial\Omega_N} \cdot \mathbf{n}_N = 0 \rightarrow (\nabla p)|_{\partial\Omega_N} \cdot \mathbf{n}_N = 0 \quad \text{on } \partial\Omega_N, \quad (6)$$

being \mathbf{n}_N the normal at the fixed boundary $\partial\Omega_N$, C the local curvature of the free boundary $\partial\Omega_T(t)$, p_0 the constant pressure in the outer healthy domain and σ_b the surface tension at the moving interface. The surface tension σ_b arises from the collective adhesive interaction among tumour cells at the MCTS boundary, primarily mediated by cadherins,⁵⁹ and from the differential contractility between the cell-cell and cell-medium interfaces, mainly mediated by α -catenin⁶⁰. Even if, in principle the surface tension σ_b depends on the density of cells, the distribution of cadherins and the presence of α -catenin⁶⁰, we will assume that it can be considered constant, for the chosen cellular population composing the aggregate.

For what concerns the chemical species, in absence of an interfacial structure, the continuity for the nutrient concentration and flux can be assumed (both in $\partial\Omega_T(t)$ and in $\partial\Omega_N$), and the concentration at the outer boundary can be assumed constant (to model the source of nutrients from the external vascular network), so that

$$n|_{\partial\Omega} = n_{out} \quad \text{on } \partial\Omega, \quad (7)$$

$$[[n]]|_{\partial\Omega_T} = 0, \quad [[\nabla n]]|_{\partial\Omega_T} \cdot \mathbf{n} = 0 \quad \text{on } \partial\Omega_T, \quad (8)$$

$$[[n]]|_{\partial\Omega_N} = 0, \quad [[\nabla n]]|_{\partial\Omega_N} \cdot \mathbf{n}_N = 0 \quad \text{on } \partial\Omega_N, \quad (9)$$

where \mathbf{n} is the outward normal vector at the boundary $\partial\Omega_T$ and $[[(\cdot)]]|_{\partial\Omega_j}$ denotes the jump of the quantity between brackets across the boundary $\partial\Omega_j$, with $j = N, T$. Finally, the compatibility condition at the free interface imposes

$$\frac{d\mathbf{x}_{\partial\Omega_T}}{dt} \cdot \mathbf{n} = \mathbf{v}_{\partial\Omega_T} \cdot \mathbf{n} \quad \text{on } \partial\Omega_T. \quad (10)$$

In the following we will work with dimensionless equations, obtained writing the system of Eqs. (1)-(4) in terms

of the dimensionless chemical concentration, $\bar{n} = n/n_c$, and the dimensionless pressure, $\bar{p} = p/p_c$ and referring to the geometry outlined in Fig. 2. The dimensionless quantities are obtained using the following characteristic time t_c , length l_c , velocity v_c , pressure p_c and chemical concentration n_c : $t_c = \gamma_n^{-1}$, $l_c = \sqrt{D_n \gamma_n^{-1}}$, $v_c = \sqrt{D_n \gamma_n}$, $p_c = D_n K_p^{-1}$, $n_c = n_{out}$. Finally, the resulting dimensionless systems of equations reads

$$\dot{\bar{n}} = \begin{cases} \bar{\nabla}^2 \bar{n} & \text{for } \bar{r} < \bar{R}_N \\ \bar{\nabla}^2 \bar{n} - \bar{n} & \text{for } \bar{R}_N < \bar{r} < \bar{R}_T(t) \\ \bar{\nabla}^2 \bar{n} & \text{for } \bar{R}_T(t) < \bar{r} < \bar{R}_{out} \end{cases} \quad (11a)$$

$$\bar{\nabla}^2 \bar{p} = -\beta \bar{\nabla}^2 \bar{n} \quad \text{for } \bar{R}_N < \bar{r} < \bar{R}_T(t) \quad (11b)$$

$$[[\bar{n}]]|_{\bar{R}_N} = 0, \quad [[\bar{\nabla} \bar{n}]]|_{\bar{R}_N} \cdot \bar{\mathbf{n}}_N = 0, \quad (\bar{\nabla} \bar{p}) \cdot \bar{\mathbf{n}}_N = 0 \quad \text{for } \bar{r} = \bar{R}_N \quad (11c)$$

$$[[\bar{n}]]|_{\bar{R}_T} = 0, \quad [[\bar{\nabla} \bar{n}]]|_{\bar{R}_T} \cdot \bar{\mathbf{n}} = 0, \quad \bar{p} = \bar{p}_0 - \bar{\sigma} \bar{C} \quad \text{for } \bar{r} = \bar{R}_T(t) \quad (11d)$$

$$\bar{n}(\bar{t}, \bar{R}_{out}) = 1 \quad \text{for } \bar{r} = \bar{R}_{out} \quad (11e)$$

$$\frac{d\bar{\mathbf{x}}_{\bar{R}_T}}{d\bar{t}} \cdot \bar{\mathbf{n}} = \bar{\mathbf{v}}_{\bar{R}_T} \cdot \bar{\mathbf{n}} = -\bar{\nabla} \bar{p}|_{\bar{R}_T} \cdot \bar{\mathbf{n}} \quad \text{for } \bar{r} = \bar{R}_T(t). \quad (11f)$$

The nondimensionalization leads to the definition of five dimensionless parameters, classified into two broad categories:

- $\beta := \chi n_c / D_n$ and $\sigma := \sigma_b K_p \gamma_n^{1/2} D_n^{-3/2} = \sigma_b K_p l_c^{-1/2} D_n^{-1}$ define mechano-biology effect on the aggregate expansion, and are called *motility* parameters;
- \bar{R}_N , \bar{R}_T and \bar{R}_{out} (*i.e.* the dimensionless radii of the necrotic core, of the MCTS and the whole domain, respectively) define the geometrical properties of the system with respect to the diffusive length l_c , and are denoted as *size* parameters.

In particular, the dimensionless parameter β represents the chemical effects associated to the expansion of MCTSs, since it can be regarded as the ratio between the typical time-scales of mass production over nutrient diffusion. On the other hand, the parameter σ defines the influence of mechanical cues over tumour development, representing the ratio of the surface tension of the aggregate over the characteristic viscous pressure of the fluid ensemble. For sake of simplicity, in the following we will omit the barred notation to denote dimensionless quantities, e.g. R_T stands for \bar{R}_T and so on.

3 Linear stability analysis of the quasi-static solution

In this Section, we first derive the quasi-static solution of the proposed model in order to mimic the early avascular

257 growth. We later perform a linear stability analysis to in-
 258 vestigate the occurrence of a morphological instability at
 259 later growth stages.

260 3.1 Quasi-stationary solution

261 At early stages of avascular growth MCTSs maintain a
 262 spherical shape^{1,3,5}. Thus, we look for a radially symmet-
 263 ric quasi-stationary solution, assuming that the diffusive
 264 process is much faster than the MCTS expansion, so that
 265 it is possible to drop the time derivative in Eq. (11a).
 266 This assumption is valid in many biological conditions,
 267 since a fast-growing tumour may expand at a rate of up
 268 to 0.5 mm/day, whereas a typical diffusion time scale is
 269 about 1 min (considering a typical length scale $L \approx 10^{-2}$ cm
 270 and a typical diffusion coefficient $D \approx 10^{-6}$ cm²s⁻¹)¹¹.
 271 Thus, it is clear that the diffusion timescale of nutrients
 272 is much shorter than the growth timescale, so that the
 273 quasi-stationary assumption can be effectively formulated.
 274 Furthermore for such long time scale the MSC can be ac-
 275 tually treated as a viscous fluid.
 276 Specializing our analysis to the case of a spherical tu-
 277 mour of radius R_T , we will denote with $n^* = n^*(r, t)$
 278 the quasi-stationary solution of Eq. 11a and with $p^* =$
 279 $p^*(r, t)$ the quasi-stationary pressure field satisfying (11b).
 280 Given the boundary conditions (11c)-(11d)-(11e) and con-
 281 sidering that n^* and p^* should be bounded, the quasi-
 282 stationary fields read

$$n^* = \begin{cases} \frac{2R_{out}e^{R_T+R_N}}{e^{2R_T}w_T^+ - e^{2R_N}w_T^-} & \text{if } r \leq R_N \\ -\frac{e^{2R_N}[e^{2(r-R_N)}(R_N+1)R_{out} + (R_N-1)R_{out}]}{r w_T^- e^{r-R_T+2R_N} - r w_T^+ e^{r+R_T}} & \text{if } R_N < r \leq R_T \\ \frac{R_{out}[e^{2R_T}(R_N+1)(r-R_T+1) - e^{2R_N}(R_N-1)(r-R_T-1)]}{r(e^{2R_T}w_T^+ - e^{2R_N}w_T^-)} & \text{otherwise} \end{cases} \quad (12)$$

$$p^* = p_0 + \frac{\sigma}{R_T} + \beta(n_{R_T}^* - n^*), \quad (13)$$

283 where we called $n_{R_T}^* = n^*(R_T)$ the concentration of the
 284 nutrient at the boundary of the aggregate and we defined
 285 $w_T^+ = (R_N+1)(R_{out}-R_T+1)$ and $w_T^- = (R_N-1)(R_{out}-$
 286 $R_T-1)$, being $w_T = (R_{out}-R_T)$ the width of the region
 287 occupied by the tumour. Then, using Eq. (11f), it is possi-
 288 ble to compute the quasi-stationary velocity of the front,
 289 which is directed along the radial direction for symmetry
 290 considerations, *i.e.* $\mathbf{v}^* = v_r^* \mathbf{e}_r$, with

$$v_r^*(R_T) = \beta \frac{R_{out}(e^{2R_N}(R_N-1)(R_T+1) - (R_N+1)e^{2R_T}(R_T-1))}{R_T^2(e^{2R_N}(R_N-1)(w_T^-) - (R_N+1)e^{2R_T}(w_T^+))}. \quad (14)$$

291 Equation (14) can be integrated numerically to determine
 292 the evolution of the spheroid border over time. The re-
 293 sult, reported in Fig. 3 for different value of the param-
 294 eter β , highlights the existence of an initial phase in which
 295 the growth of the aggregate is nearly exponential and a
 296 subsequent one in which the expansion of the tumour is
 297 almost linear, as observed in^{32,61}. Indeed, in standard
 298 MCTS free-growth (*i.e.* without the introduction of an
 299 external stress) in liquid suspension or at moderate agaros-
 300 is gel concentration, the plot of the tumor diameter over

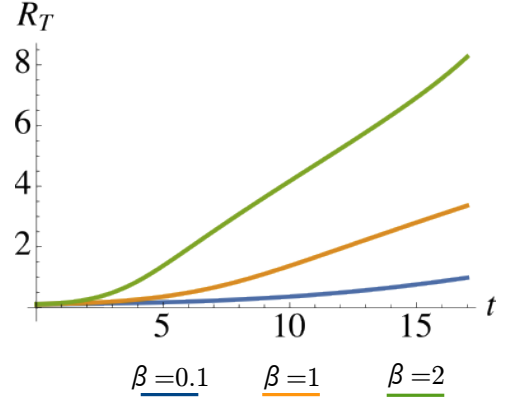


Figure 3. Quasi-stationary solution of the proposed model, depicting the radius of the tumour over time for different values of the motility parameter β . At early stages the growth is exponential, as a consequence of the bulk availability of nutrients. At later stages, the growth law is almost linear, reflecting the higher nutrient concentration on the outer surface of the growing spheroid.

301 time exhibits an early stage of exponential growth, cor-
 302 responding to spheroid volumetric growth, since nutrients
 303 are available everywhere in the spheroid bulk^{32,61}. Subse-
 304 quently, when the diameter of the spheroid becomes much
 305 larger than the penetration length of the nutrient, the cel-
 306 lular growth becomes mainly localized on the surface of
 307 the tumor, leading to a linear growth in time.

308 3.2 Perturbation of the quasi-stationary solution

309 In this paragraph, we investigate the stability of the steady,
 310 radially-symmetric solution by applying small perturba-
 311 tions of the MCTS boundary.

312 Let R_T^* be the unperturbed position of the moving inter-
 313 face, we consider a small perturbation ($\varepsilon \ll 1$) of the kind

$$R(\theta, \varphi, t) = R_T^*(t) + \varepsilon e^{\lambda t} \text{Re} [Y_\ell^m(\theta, \varphi)]. \quad (15)$$

314 where $\lambda \in \mathbb{R}$ is the *amplification rate* (or *time-growth rate*)
 315 of the perturbation and $Y_\ell^m(\theta, \varphi)$ is the spherical harmonic
 316 of *degree* ℓ and *order* m , with $m \in \mathbb{N}$, $\ell \in \mathbb{N}^+$ and $|m| \leq \ell$.
 317 The spherical harmonics $Y_\ell^m(\theta, \varphi)$ form a complete set
 318 of orthonormal functions and thus any square-integrable
 319 function can be expanded as a linear combination of spheri-
 320 cal harmonics. For physical consistency, the variations of
 321 n and p from the quasi-stationary solutions n^* and p^*
 322 should be in the form

$$n(r, \theta, \varphi, t) = n^*(r, t) + \varepsilon n_1(r) e^{\lambda t} \text{Re} [Y_\ell^m(\theta, \varphi)] \quad (16)$$

$$p(r, \theta, \varphi, t) = p^*(r, t) + \varepsilon p_1(r) e^{\lambda t} \text{Re} [Y_\ell^m(\theta, \varphi)], \quad (17)$$

323 Using Eq. (11a) and the relation $\nabla_\Omega^2 Y_\ell^m + \ell(\ell+1)Y_\ell^m = 0$,
 324 where we set the angular part of the Laplacian operator as
 $\nabla_\Omega^2(\cdot) = 1/\sin\theta \partial/\partial\theta(\sin\theta \partial(\cdot)/\partial\theta) + 1/\sin^2\theta \partial^2(\cdot)/\partial\phi^2$,
 the term n_1 must obey the following ODE

$$r^2 n_1''(r) + 2r n_1'(r) - (\ell(\ell+1) + (\lambda + \mathbf{1}_{\Omega_T})r^2) n_1(r) = 0, \quad (18)$$

where primes denote derivatives on r and $\mathbf{1}_{\Omega_T} = 1$ if $R_N < r \leq R_T^*$, $\mathbf{1}_{\Omega_T} = 0$ otherwise. The solution of Eq. (18), for $\lambda \neq \{0, -1\}$ is

$$n_1(r) = \begin{cases} C_1 i_\ell(\sqrt{\lambda}r) & \text{if } r \leq R_N \\ B_1 i_\ell(\sqrt{\lambda+1}r) + B_2 k_\ell(\sqrt{\lambda+1}r) & \text{if } R_N < r \leq R_T^* \\ A_1 i_\ell(\sqrt{\lambda+1}r) + A_2 k_\ell(\sqrt{\lambda+1}r) & \text{if } R_T^* < r \leq R_{out}, \end{cases} \quad (19)$$

where $i_\ell(r)$ and $k_\ell(r)$ are the modified spherical Bessel function of the first and second kind, respectively, evaluated in r . The coefficients A_1, A_2, B_1, B_2, C_1 appearing in the expression of $n_1(r)$ can be determined imposing the incremental boundary conditions for the concentration field (11c), (11d) and (11e), being

$$\llbracket n_1 \rrbracket|_{R_N} = 0, \quad \left[\left[\frac{\partial n_1}{\partial r} \right] \right]_{R_N} = 0, \quad (20)$$

$$\llbracket n_1 \rrbracket|_{R_T^*} = 0, \quad \left[\left[\frac{\partial n_1}{\partial r} \right] \right]_{R_T^*} = n_0, \quad n_1(R_{out}) = 0. \quad (21)$$

The perturbed pressure field p_1 in Ω_T is obtained from Eq.(11b) that leads to

$$p_1(r) = Qr^\ell + Wr^{-\ell-1} - \beta(B_1 i_\ell(\sqrt{\lambda+1}r) + B_2 k_\ell(\sqrt{\lambda+1}r)) \quad (22)$$

where the constants Q and W can be determined from the boundary conditions on the pressure field (11c) and (11d), considering only the first order terms, *i.e.*

$$p_1(R_T^*) = -\sigma \frac{2}{R_T^{*2}} (2 - (\ell + 1)\ell) - \frac{\partial p^*}{\partial r}|_{R_T^*}, \quad \frac{\partial p_1}{\partial r}|_{R_N} = 0 \quad (23)$$

perturbation theory⁶² Finally, using standard procedures in perturbation theory⁶², imposing the boundary condition (10) at the perturbed interface and neglecting the terms of order higher than the first in the series expansion, it is possible to obtain the following dispersion equation

$$\lambda = -p^{*''}(R_T^*) - p_1'(R_T^*), \quad (24)$$

which has the same form of the relation found for the rectilinear front on an infinite domain⁶³ or an expanding circular colony^{64,65}. The dispersion equation (24) is an implicit function of the time-growth mode λ and the spherical harmonic degree ℓ , depending on the five dimensionless parameters $\beta_i, \sigma, R_N, R_T^*$ and R_{out} . Interestingly, λ does not depend on the azimuthal component of the model solutions $Y_\ell^m(\phi, \theta)$, *i.e.* the solutions are independent of the order m , as observed also in previous works based on different models^{15,50}.

4 Results and Discussion

The dispersion equation (24) has been solved numerically in order to investigate the global stability of the solutions depending on the system parameters. The corresponding dispersion diagrams are reported in Fig. 4 for different values of both the size and the motility parameters. As

in classical perturbation theory⁶², a positive real part of the growth rate λ implies global instability, thus highlight a critical spatial mode of the perturbation defined by the degree ℓ associated with the highest positive growth rate. Interestingly, Fig. 4 shows that the spheroid front is linearly unstable at small ℓ , with $\ell = 1$ being always unstable. Indeed, whilst for a spheroid growing inside an infinite homogeneous domain with constant chemical concentration, one would expect to find $\lambda = 0$ for $\ell = 1$, due to translational symmetry^{11,15,50}, we must remind that in our case, due to the presence of the external environment the translational symmetry is no longer preserved.

Furthermore, the dispersion diagrams in Fig. 4 also indicate the emergence of a characteristic mode different from $\ell = 1$ in the cases of bigger size parameters (see Fig. 4-a), as well as of small values of the motility parameters σ (see Fig. 4-c) and β (see Fig. 4-d). Interestingly, the characteristic mode is not significantly affected by varying only the dimension of the external domain, while keeping the necrotic radius R_N and the initial tumour radius R_T fixed (Fig. 4-b) Moreover, whether the range of unstable modes is highly influenced by the sizes parameters and by the motility parameter σ (Fig. 4-a-c), it is not deeply influenced by variations of R_{out} and β (Fig. 4-b-d). Indeed as either the size of the domains decreases (Fig. 4-a) or σ increases, the range of unstable modes decreases, up to a range where only $\ell = 1$ is unstable. The dependency on the size of the domains states that smaller diffusive lengths (*i.e.* smaller diffusion coefficient or higher absorption rate of the nutrients) lead to highly irregular contours during the growth of the tumour. On the other hand, the effect on the mechanical parameter σ on the dispersion diagram shows that, as expected, the surface tension σ_b , along with an high permeability of the surrounding porous environment k act a stabilizing effect on the front (see Fig. 4-c), whereas the viscosity of the tumour cluster destabilize the border of the MCTS leading to more aggressive tumours. As β settles the velocity of the quasi-stationary moving front (see Eq. (14)), the dispersion diagram in Fig. 4-d shows that the tumour developed highly irregular contour only in the case of slowly-moving front (*i.e.* small chemotactic coefficient and proliferation), since for fast moving front the characteristic mode decrease, until only $\ell = 1$ is unstable.

Moreover, it is interesting to consider the role played by the radius of the growing tumour in the development of instabilities, while keeping all the other parameters fixed (see Fig. 5). Fig. 5-a reports the results for a set of parameters R_{out}, R_N, β and σ for which, independently from R_T , the most unstable mode is always $\ell = 1$. This situation corresponds to a sort of translation of the spheroid inside the domain (see Fig. 5-a on the right). On the other hand, the characteristic mode depends on the MCTS size in a certain range of material parameters (see Fig. 5-b). Indeed, it increases for increasing R_T , so that bigger tumours show more irregularities at their border. Therefore, a growing MCTS can undergo a morphological transition that may significantly affect the invasion pattern towards

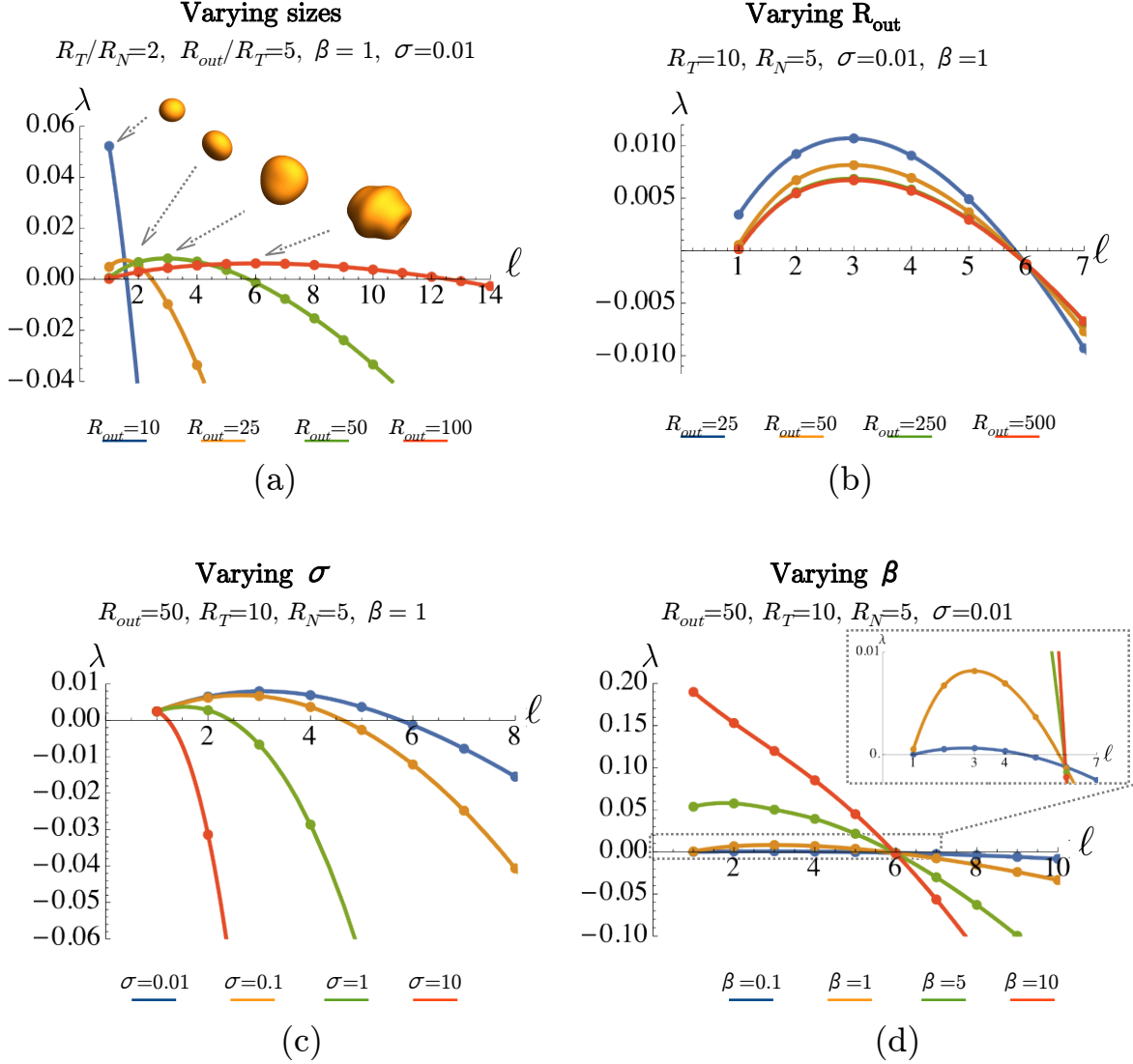


Figure 4. Dispersion diagrams for different values of the model parameters (a) R_{out} keeping $q = R_{out}/R_N$ constant, (b) R_{out} keeping R_N constant, (c) σ and (d) β . The solid lines in the graphs are obtained by interpolating the discrete values (see the dots on the curves) of the time growth rate of the perturbation, λ , calculated for integer values of ℓ from eq. (24). In (a) the shapes of the tumour corresponding to the characteristic mode ($\ell = 1, 2, 3, 6$) is reported.

420 the typical finger-like structures observed for invasive car- 434
 421 cinomas (see Fig. 5-b). 435

422 Finally, Fig. 6 depicts the perturbed pressure and ve- 436
 423 locity fields for a linearly unstable perturbation, given by 437
 424 a spherical harmonic of the kind $Y_{10}^6(\theta, \varphi)$. The highest 438
 425 variation of the pressure is located in a thin shell closer 439
 426 to the interface of the tumour, so that in the bulk of the 440
 427 tumour the velocity is almost null. In the region just at 441
 428 the rear of small protrusions (due to the perturbation of 442
 429 the boundary), the pressure field increases, so that the 443
 444 velocity at the border of the MCTS where a protrusion 445
 446 form, for the unstable modes (such as the one reported 446
 447 in Fig. 6), is higher than the velocity in the invagination 447
 on the contour. Furthermore, from the perturbed field it

434 is possible to appreciate small negative radial velocities in 434
 435 the bulk, just at the rear of the region where protrusion 435
 436 forms. Thus, while the spheroid surface moves outward, 436
 437 some cells inside the cluster move inward. This result con- 437
 438 firms the existence of a radial convergent flow, in addition 438
 439 to the divergent flow that makes the aggregate expand, as 439
 440 pointed out in^{66,67}. This effect combined with the higher 440
 441 velocity associated to the protrusion border could explain 441
 the possible detachment of carcinoma cells that lead to 442
 metastasis and thus the higher invasivity of tumours with 443
 irregular contours.

442 Even though the onset of irregular contours and the de- 442
 443 velopment of a retrograde flow are in qualitative agree- 443
 444 ment with biological experiments⁶⁶⁻⁶⁸, a direct quantita- 444
 445 tive analysis is needed. 445

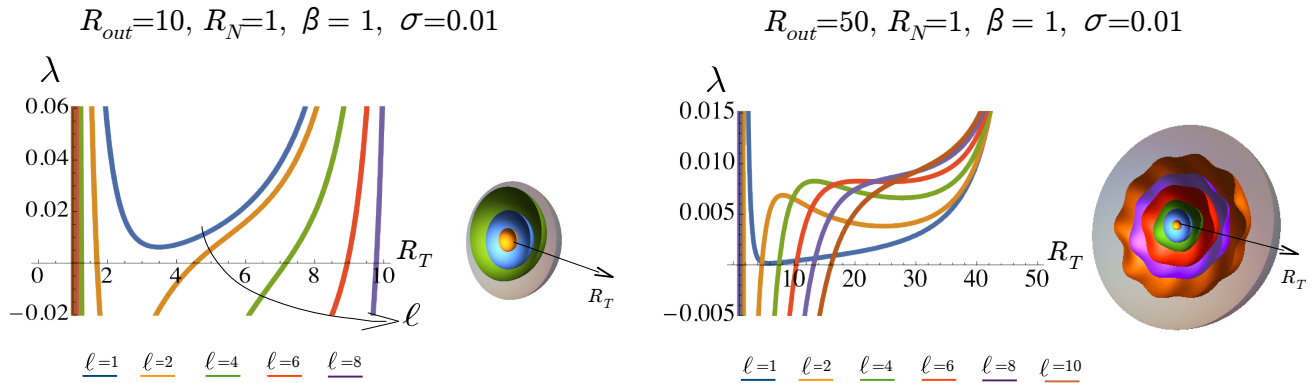


Figure 5. Evolution of the time growth rate of the perturbation λ with respect to the dimensionless tumour radius, R_T , for different values of ℓ (with $\ell = 1, 2, 4, 6, 8, 10$). (a) For the chosen set of parameters, $\ell = 1$ is the most unstable mode, whatever the tumour radius is. The deformed shapes corresponding to $R_T = 2, 5, 8$ are reported aside (the gray region represents the outer environment). (b) The characteristic mode ℓ changes for different values of the tumour radius. Aside the dispersion curves, the section of the tumour perturbed shapes are reported for $R_T = 2.5, 8, 12.5, 20, 26, 35$ to which the corresponding characteristic modes are $\ell = 1, 2, 4, 6, 8, 10$ respectively.

448 tive comparison between our predictions and the biological experiments is not straightforward. First, not all the data required by the mathematical model, even though measurable in principle, are reported in literature. Second, most of the work in the vast literature on MCTSs focus on the effect of nutrients availability and stress on the growth of the spherical tumor aggregate, whereas little attention have been paid on the systematic mapping of contour instabilities onset and evolution. Therefore, further morphological data on MCTS, combined with estimates of the underlying biological parameters involved in the process (i.e. nutrients diffusion and uptake, surface tension of the aggregate and permeability of the porous medium), are highly required for the future validation of the proposed model.

463 5 Conclusions

464 In this work we have presented a continuum model for describing the avascular growth of a multicellular tumour spheroid, comprising a fixed necrotic core surrounded by a region of proliferative cells, guided by the uptake of a diffusing nutrient. The proposed model encapsulates the diffusion of a chemical species from the vasculature of the healthy region and the tumour cell response to nutrients, via their proliferation and their chemotactic migration inside the extracellular space. The proposed model differs from existing approaches^{2,49,50} since it considers a growth though a rigid, porous surrounding material. Moreover, the MCTS expansion is guided not only by cell proliferation as in^{2,49,50}, but also by the chemotactic motion of cells, through a non-convective mass flux term. Differently from^{2,50}, that assumed a Gibbs-Thompson relation⁶⁹ on the moving boundary for the chemical potential, we considered a mechanical effect in term of a surface tension at the MCTS outer boundary, leading to the Young-Laplace equation at the interface.

The proposed model is governed by five dimensionless parameters: two of them, β and σ are called motility parameters and representing the mechano-biology cues, the other three are denoted size parameters and are related to the typical sizes of the domains with respect to the diffusive length. The analytic results predicted the existence of a quasi-stationary radially-symmetric tumour configuration that is always linearly unstable to asymmetric perturbations involving spherical harmonics $Y_\ell^m(\theta, \phi)$, with the range of the unstable modes depending on the dimension of the domain with respect to the diffusive length and on the motility parameter β , related to the chemotactic growth of the tumour. We remark that, whilst a MCTS growing inside an infinite homogeneous domain is marginally stable, i.e. $\lambda = 0$ for $\ell = 1$ ^{11,15,50}, the proposed model is always linearly unstable, since translational symmetry is broken by considering a finite dimension of the surrounding media. Furthermore, differently from existing works^{2,8,9,14,15,17}, the perturbation analysis is conducted here without neglecting the diffusion timescale in the unstable growth rate.

The analysis of the perturbed field also pointed out a possible mechanism that could lead to the detachment of metastasis from the primary tumour mass, based on the development of higher velocity at the border of the MCTS and a convergent flow inside where protrusions form. This mechanism could explain why the propensity for asymmetric invasion and the installation of irregular morphology characterize the growth of aggressive carcinomas *in vivo*. Thus, this approach has the potential to foster our understanding on the process of transition from the benign to the aggressive tumour stage and might provide also some indications for improving therapeutic treatments. Indeed, more blurred and irregular contours detected *in vivo* can be related to more malignant tumour, with respect to smoother and clearer contours that can be associated to benign carcinomas.

498
499
500
501
502
503
504
505
506
507
508
509
510
511
512
513
514
515
516
517
518
519

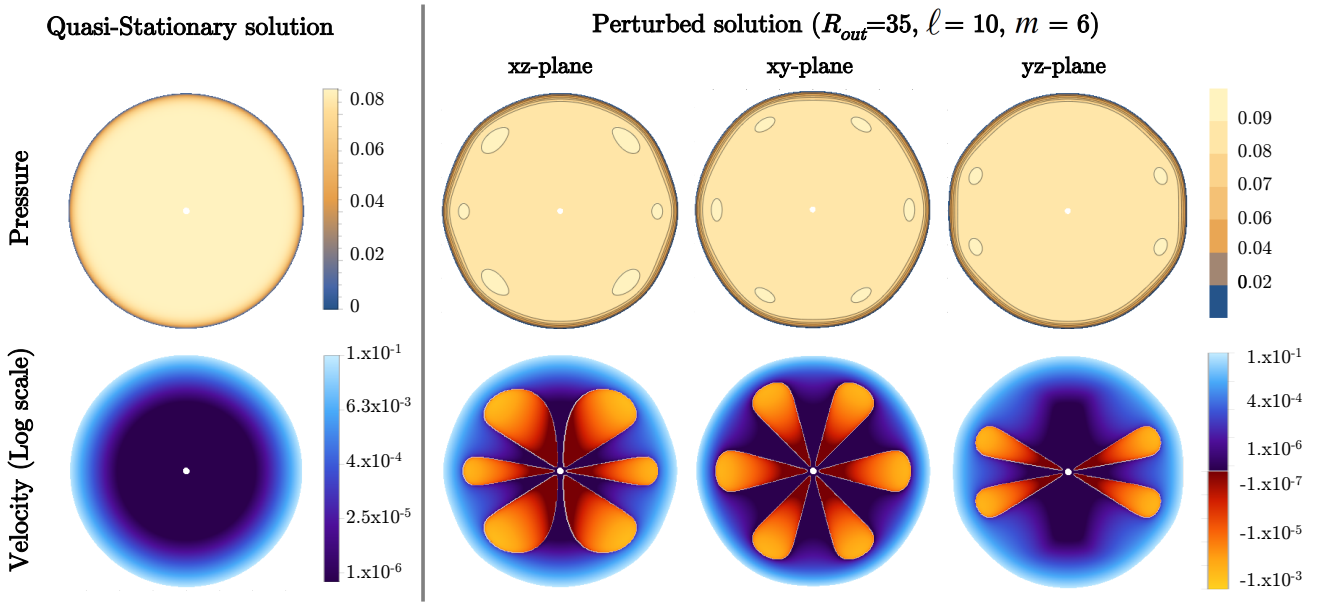


Figure 6. Evolution of the quasi-stationary and perturbed pressure and velocity fields for $R_n = 1$, $R_T^* = 35$, $R_{out} = 50$ for a perturbation of the kind $e^{\lambda t} Y_{10}^6(\theta, \varphi)$. Since higher changes in the velocity and pressure field occurs only at the interface, we use a logarithmic scale in the velocity plot in order to show small variations of the perturbed field inside the bulk of the tumour. The perturbed velocity field highlights the existence of negative radial velocities (*i.e.* radial convergent flow), as pointed out in ^{66,67}.

However, the present model considers a really simplified geometry and adopts some simplifications in order to obtain a model that can be studied analytically. Thus, future improvements of the proposed mathematical model should focus on the explicit description of quiescent cell region (that in the present model corresponds to the region of the spheroid in which we have an almost null velocity) and on tracking the evolution of the inner necrotic core occurring, for instance, when the nutrients concentration attains a specific value^{2,12} (whereas in the present work the fixed radius R_N of the necrotic core is a parameter in the sensitivity analysis). Then, the stability analysis can be enriched by considering the weakly nonlinear interactions of the asymmetric modes, as well as their evolution depending on the order m of the spherical harmonic perturbation (as done for example in¹⁵ in a simplified case) and numerical techniques should be developed in order to simulate the fully nonlinear evolution of the morphological transition.

From the modelling point of view, future studies should also consider the effect of the cells populating the surrounding healthy environment on the consumption of nutrients and the effect of varying local densities (both inside the healthy tissue and inside the different tumor regions) on the nutrient diffusion coefficient. Then, the effect of solid mechanical stresses on the growth dynamics of tumours^{32,61,67,70–73} and the effect of the possible deformation, degradation and reorganization of extracellular matrix fibres^{74–76} should be included to move towards a more realistic representation of the problem. Indeed, for tumours growing both *in vivo* and in xenograft animal models, the description of the system evolution is far more complex

than the one proposed in this work, referred to MCTS growth inside inert and rigid ECM scaffolds. In particular, it has been shown that the geometrical and mechanical properties of the ECM^{74,75} play an important role for the possible formation of metastasis, since they can lead to growth arrest (*i.e.* spheroid compartmentalization) or, on the contrary, foster the detachment of invasive cells. Along with the rigidity of the matrix, its density, and the tensile forces generated in the ECM^{74,75}, more recent studies identify the matrix pore size as the critical property modulating cancer cell invasion^{77,78}. Based on these biological observations, some recent mathematical models have been developed to take into account, on one hand, MCTS segregation by thick porous (but still rigid and homogeneous) structures^{79–81} and, on the other, ECM deformation⁸². Furthermore, not only ECM fibers can accumulate or being degraded at the host-MCTS interface, but they strongly reorganize, aligning parallel to the tumor border, in a first stage, and then perpendicular to the tumor boundary⁷⁴.

Thus, to take into account all these aspects and more realistically describe tumor growth *in vivo*, an anisotropic poro-elasto-visco-plastic model with a threshold (based on microscopic arguments) for cell motion should be developed. However in that case tumor irregular contours will likely arise for inhomogeneity and anisotropy in the ECM, whereas this work demonstrates that mechano-biological and (macroscopic) geometrical cues can determine the occurrence of a morphological transition in growing tumours that can promote invasiveness, even in an homogeneous environment. The theoretical results push towards the developments of further biological experiments for accu-

rate characterization of MCTS morphology and careful measures of the surface tension and the interstitial pressure within MCTS^{59,83}, as well as growth and mobility properties of the tumour cells to validate the predictions of the model. Indeed, the integration of mathematical tools in biological research could be crucial for estimating the tumour's ability to invade its host environment.

6 Acknowledgments

This work was funded by the "Associazione Italiana per la Ricerca sul Cancro" (AIRC) through My First AIRC Grant 17412, partially supported by the "Start-up Packages and PhD Program" project, co-funded by Regione Lombardia through the "Fondo per lo sviluppo e la coesione 2007-2013 -formerly FAS", and by the "Progetto Giovani GNFM 2016".

References

1. J. Folkman and M. Hochberg, "Self-regulation of growth in three dimensions," *The Journal of Experimental Medicine*, vol. 138, pp. 745–753, 1973.
2. H. Byrne and M. Chaplain, "Free boundary value problems associated with the growth and development of multicellular spheroids," *European Journal of Applied Mathematics*, vol. 6, pp. 639–658, 1997.
3. R. Sutherland and R. Durand, "Growth and cellular characteristics of multicell spheroids," in *Spheroids in Cancer Research* (H. Acker, J. Carlsson, R. Durand and R. M. Sutherland, eds.), vol. 95 of *Recent Results in Cancer Research*, pp. 24–49, Springer Berlin Heidelberg, 1984.
4. K. Groebe and W. Mueller-Klieser, "Distributions of oxygen, nutrient and metabolic waste concentrations in multicellular spheroids and their dependence on spheroid parameters," *European Biophysics Journal*, vol. 19, pp. 169–181, 1991.
5. R. Sutherland, "Cell and environment interactions in tumor microregions: the multicell spheroid model," *Science*, vol. 240, no. 4849, pp. 177–184, 1988.
6. J. Folkman, "Tumour angiogenesis," *Advances in Cancer Research*, vol. 19, pp. 331–358, 1974.
7. V. R. Muthukarruppan, L. Kubai, and R. Auerbach, "Tumour-induced neovascularisation in the mouse eye," *Journal of the National Cancer Institute*, vol. 69, pp. 699–705, 1982.
8. J. A. Adam, "A simplified mathematical model of tumor growth," *Mathematical Biosciences*, vol. 81, pp. 229–244, 1986.
9. J. A. Adam, "A mathematical model of tumour growth. ii. effects of geometry and spatial uniformity on stability," *Mathematical Biosciences*, vol. 86, pp. 183–211, 1987.
10. J. A. Adam and S. A. Maggelakis, "Diffusion regulated growth characteristics of a spherical prevascular carcinoma," *Bulletin of Mathematical Biology*, vol. 52, pp. 549 – 582, 1990.

11. H. Byrne and M. A. J. Chaplain, "Growth of non-necrotic tumours in the presence and absence of inhibitors," *Mathematical Biosciences*, vol. 130, pp. 151–181, 1995.
12. H. Byrne and M. A. J. Chaplain, "Growth of necrotic tumours in the presence and absence of inhibitors," *Mathematical Biosciences*, vol. 135, pp. 187–216., 1996.
13. M. A. J. Chaplain, *Experimental and Theoretical Advances in Biological Pattern Formation*, ch. The development of a spatial pattern in a model for cancer growth., pp. 45–60. Plenum Press, 1993.
14. H. P. Greenspan, "Models for the growth of a solid tumour by diffusion," *Studies in Applied Mathematics*, vol. 52, pp. 317–340, 1972.
15. H. Byrne, "A weakly nonlinear analysis of a model of avascular solid tumour growth," *Journal of Mathematical Biology*, vol. 39, no. 1, pp. 59 – 89, 1999.
16. S. A. Maggelakis and J. A. Adam, "Mathematical model of prevascular growth of a spherical carcinoma," *Mathematical and Computer Modelling*, vol. 13, pp. 23–38, 1990.
17. D. L. S. McElwain and L. E. Morris, "Apoptosis as a volume loss mechanism in mathematical models of solid tumour growth," *Mathematical Biosciences*, vol. 39, pp. 147–157, 1978.
18. D. Ambrosi and L. Preziosi, "On the closure of mass balance models for tumor growth," *Mathematical Models and Methods in Applied Sciences*, vol. 12, no. 5, pp. 737–754, 2002.
19. R. P. Araujo and D. L. S. McElwain, "A history of the study of solid tumour growth: The contribution of mathematical modeling," *Bulletin of Mathematical Biology*, vol. 66, pp. 1039–1091, 2004.
20. J. S. Lowengrub, H. B. Frieboes, F. Jin, Y. L. Chuang, X. Li, P. Macklin, S. M. Wise, and V. Cristini, "Non-linear modelling of cancer: Bridging the gap between cells and tumours," *Nonlinearity*, vol. 23, pp. R1–R91, 2010.
21. D. McElwain and G. Pettet, "Cell migration in multicell spheroids: Swimming against the tide," *Bulletin of Mathematical Biology*, vol. 55, no. 3, pp. 655–674, 1993.
22. C. Chen, H. Byrne, and J. King, "The influence of growth-induced stress from the surrounding medium on the development of multicell spheroids," *Journal of Mathematical Biology*, vol. 43, pp. 191–220, 2001.
23. K. A. Landman and C. P. Please, "Tumour dynamics and necrosis: surface tension and stability," *Mathematical Medicine and Biology*, vol. 18, no. 2, pp. 131–158, 2001.
24. M. Steinberg, "Reconstruction of tissues by dissociated cells. some morphogenetic tissue movements and the sorting out of embryonic cells may have a common explanation," *Science*, vol. 141, no. 3579, pp. 401–408, 1963.
25. R. Foty, G. Forgacs, C. Pfelegerand, and M. Steinberg, "Liquid properties of embryonic tissues: Measurement of interfacial tensions," *Physical Review Letters*

- ters, vol. 72, no. 14, pp. 2298–2301, 1994.
- 697 26. G. Forgacs, R. Foty, Y. Shafir, and M. Steinberg, 755
698 “Viscoelastic properties of living embryonic tissues: 756
699 a quantitative study,” *Biophysical Journal*, vol. 74, 757
700 no. 5, pp. 2227–2234, 1998. 758
- 701 27. G. Vitale and L. Preziosi, “A multiphase model 759
702 of tumor and tissue growth including cell adhesion 760
703 and plastic reorganization,” *Mathematical Models and 761
704 Methods in Applied Sciences*, vol. 21, no. 9, pp. 1901– 762
705 1932, 2011. 763
- 706 28. M. A. J. Chaplain and B. D. Sleeman, “Modelling 764
707 the growth of solid tumours and incorporating a 765
708 method for their classification using nonlinear elastic- 766
709 ity theory,” *Journal of Mathematical Biology*, vol. 31, 767
710 pp. 431–473, 1993. 768
- 711 29. R. Skalak, S. Zargaryan, R. K. Jain, P. A. Netti, and 769
712 A. Hoger, “Compatibility and the genesis of residual 770
713 stress by volumetric growth,” *Journal of Mathemat- 771
714 ical Biology*, vol. 34, pp. 889–914, 1996. 772
- 715 30. D. Ambrosi and F. Mollica, “The role of stress in the 773
716 growth of a multicell spheroid,” *Journal of Mathemat- 774
717 ical Biology*, vol. 48, no. 5, pp. 477–499, 2004. 775
- 718 31. T. Roose, P. A. Netti, L. L. Munn, Y. Boucher, and 776
719 R. K. Jain, “Solid stress generated by spheroid growth 777
720 estimated using a linear poroelasticity model,” *Mi- 778
721 crovascular Research*, vol. 66, no. 3, pp. 204–212, 2003. 779
- 722 32. C. Voutouri, F. Mpekris, P. Papageorgis, A. Odysseos, 780
723 and T. Stylianopoulos, “Role of constitutive behavior 781
724 and tumor-host mechanical interactions in the state of 782
725 stress and growth of solid tumors,” *PLoS ONE*, vol. 9, 783
726 no. 8, p. e104717, 2014. 784
- 785 33. R. Vandiver and A. Goriely, “Morpho-elastodynamics 786
787 The long-time dynamics of elastic growth,” *Journal of 788
789 Biological Dynamics*, vol. 3, pp. 180–195, 2009. 789
- 790 34. T. Stylianopoulos, J. D. Martin, V. P. Chauhan, S. R. 790
791 Jain, B. Diop-Frimpong, N. Bardeesy, B. L. Smith, 791
792 C. R. Ferrone, F. J. Hornicek, Y. Boucher, L. L. Munn, 792
793 and R. K. Jain, “Causes, consequences, and remedies 793
794 for growth-induced solid stress in murine and human 794
795 tumors,” *PNAS*, vol. 109, no. 38, pp. 15101–15108, 795
2012. 796
- 797 35. D. Ambrosi and L. Preziosi, “Cell adhesion mecha- 797
798 nisms and stress relaxation in the mechanics of tu- 798
799 mours,” *Biomechanics and Modeling in Mechanobiol- 799
800 ogy*, vol. 8, pp. 397–413, 2009. 800
- 801 36. D. Ambrosi, L. Preziosi, and G. Vitale, “The inter- 801
802 play between stress and growth in solid tumors,” *Mech- 801
803 anics Research Communications*, vol. 42, pp. 87–94, 802
2012. Recent Advances in the Biomechanics of Growth 803
and Remodeling. 804
- 805 37. C. Giverso, M. Scianna, and A. Grillo, “Growing avas- 805
806 cular tumours as elasto-plastic bodies by the theory of 805
807 evolving natural configurations,” *Mechanics Research 806
808 Communications*, vol. 68, pp. 31–39, 2015. 808
- 809 38. B. Aigouy, R. Farhadifar, D. Staple, A. Sagner, 809
810 J. Röper, F. Jülicher, and S. Eaton, “Cell flow reori- 810
811 ents the axis of planar polarity in the wing epithelium 811
812 of drosophila,” *Cell*, vol. 142, no. 5, pp. 773–786, 2010. 812
- 813 39. T. Vasilica Stirbat, S. Tlili, T. Houver, J. P. Rieu, 755
C. Barentin, and H. Delanoë-Ayari, “Multicellular ag- 756
gregates: a model system for tissue rheology,” *The Eu- 757
ropean Physical Journal E*, vol. 36, no. 8, pp. 1–14, 758
2013. 759
40. J. Ranft, M. Basan, J. Elgeti, J. Joanny, J. Prost, and 760
F. Jülicher, “Fluidization of tissues by cell division 761
and apoptosis,” *PNAS*, vol. 107, no. 49, pp. 20863– 762
20868, 2010. 763
41. J. J. Casciari, S. V. Sotirchos, and R. M. Sutherland, 764
“Mathematical modelling of microenvironment and 765
growth in emt6/r0 multicellular tumour spheroids,” 766
Cell Proliferation, vol. 25, pp. 1–22, 1992. 767
42. M. Marusic, Z. Bajzer, J. P. Freyer, and S. Vuk- 768
Pavlovic, “Analysis of growth of multicellular tumour 769
spheroids by mathematical models,” *Cell Prolifera- 770
tion*, vol. 27, pp. 73–94, 1994. 771
43. R. Muir, *Muir’s Textbook of Pathology*. CRC Press, 772
15th edn ed., 2012. 773
44. S. S. Cross and D. W. K. Cotton, “The fractal dimen- 774
sion may be a useful morphometric discriminant in 775
histopathology,” *The Journal of Pathology*, vol. 166, 776
pp. 409–411, 1992. 777
45. S. S. Cross, J. P. Bury, P. B. Silcocks, T. J. Stephen- 778
son, and D. W. K. Cotton, “Fractal geometric anal- 779
ysis of colorectal polyps,” *The Journal of Pathology*, 780
vol. 172, pp. 317–323, 1994. 781
46. G. Landini and J. W. Rippin, “How important is tu- 782
mour shape?,” *The Journal of Pathology*, vol. 179, 783
pp. 210–17, 1996. 784
47. R. Sutherland and R. E. Durand, “Radiation response 785
of multicell spheroids: An in vitro tumour model,” 786
International Journal of Radiation Biology, vol. 23, 787
pp. 235–246, 1973. 788
48. M. Tubiana, “The kinetics of tumour cell proliferation 789
and radiotherapy,” *The British Journal of Radiology*, 790
vol. 44, pp. 325–347, 1971. 791
49. H. P. Greenspan, “On the growth and stability of cell 792
cultures and solid tumours,” *Journal of Theoretical 793
Biology*, vol. 56, pp. 229–242, 1976. 794
50. H. Byrne and M. Chaplain, “Modelling the role of 795
cell-cell adhesion in the growth and development of 796
carcinomas,” *Mathematical and Computer Modelling*, 797
vol. 24, no. 12, pp. 1–17, 1996. 798
51. M. Espinosa, G. Ceballos-Cancino, R. Callaghan, 799
V. Maldonado, N. Patiño, V. Ruíz, and J. Meléndez- 800
Zajgla, “Survivin isoform delta ex3 regulates tumor 801
spheroid formation,” *Cancer Letters*, vol. 318, no. 1, 802
pp. 61–67, 2012. 803
52. A. Nyga, U. Cheema, and M. Loizidou, “3D tumour 804
models: novel in vitro approaches to cancer studies,” 805
Journal of Cell Communication and Signaling, vol. 5, 806
pp. 239–248, 2011. 807
53. S. Wise, J. Lowengrub, H. Frieboes, and V. Cristini, 808
“Three-dimensional multispecies nonlinear tumor 809
growth—I Model and numerical method,” *Journal of 810
Theoretical Biology*, vol. 253, no. 3, pp. 524–543, 2008. 811
54. A. Ramanathan, C. Wang, and S. Schreiber, “Pertur- 812
bational profiling of a cell-line model of tumorigenesis 813

- by using metabolic measurements,” *PNAS*, vol. 102, no. 17, pp. 992–7, 2005.
55. H. Byrne and L. Preziosi, “Modelling solid tumour growth using the theory of mixtures,” *Mathematical Medicine and Biology*, vol. 20, pp. 341–366, 2003.
56. K. J. Painter, “Continuous models for cell migration in tissues and applications to cell sorting via differential chemotaxis,” *Bulletin of Mathematical Biology*, vol. 71, no. 5, pp. 1117–1147, 2009.
57. E. T. Roussos, J. S. Condeelis, and A. Patsialou, “Chemotaxis in cancer,” *Nature Reviews Cancer*, vol. 11, no. 8, pp. 573–587, 2011.
58. E. Keller and L. Segel, “Model for chemotaxis,” *Journal of Theoretical Biology*, vol. 30, pp. 225–234, 1971.
59. A. Fathi-Azarbayjani and A. Jouyban, “Surface tension in human pathophysiology and its application as a medical diagnostic tool,” *Bioimpacts*, vol. 5, no. 1, pp. 29–44, 2015.
60. T. Stirbat, A. Mgharbel, S. Bodenec, K. Ferri, H. Mertani, J.-P. Rieu, and H. Delanoë-Ayari, “Fine Tuning of Tissues’ Viscosity and Surface Tension through Contractility Suggests a New Role for α -Catenin,” *PLoS ONE*, vol. 8, no. 2, p. e52554, 2013.
61. G. Helmlinger, P. A. Netti, H. C. Lichtenbeld, R. J. Melder, and R. K. Jain, “Solid stress inhibits the growth of multicellular tumor spheroids,” *Nature Biotechnology*, vol. 15, no. 8, pp. 778–783, 1997.
62. A. Nayfeh, *Perturbation Methods*. John Wiley and Sons, 2000.
63. P. Ciarletta, “Free boundary morphogenesis in living matter,” *European Biophysics Journal*, vol. 41, pp. 681–686, 2012.
64. C. Giverso, M. Verani, and P. Ciarletta, “Branching instability in expanding bacterial colonies,” *Journal of The Royal Society Interface*, vol. 12, no. 104, 2015.
65. C. Giverso, M. Verani, and P. Ciarletta, “Emerging morphologies in round bacterial colonies: comparing volumetric versus chemotactic expansion,” *Biomchanics and Modeling in Mechanobiology*, pp. 1–19, 2015.
66. M. Dorie, R. Kallman, D. Rapacchietta, D. Van Antwerp, and Y. Huang, “Migration and internalization of cells and polystyrene microspheres in tumor cell spheroids,” *Experimental Cell Research*, vol. 141, no. 1, pp. 201–209, 1982.
67. M. Delarue, F. Montel, O. Caen, J. Elgeti, J. M. Siaugue, D. Vignjevic, J. Prost, J. F. Joanny, and G. Cappello, “Mechanical control of cell flow in multicellular spheroids,” *Physical Review Letters*, vol. 110, p. 138103, 2013.
68. H. Frieboes, X. Zheng, C.-H. Sun, B. Tromberg, R. Gatenby, and V. Cristini, “An integrated computational/experimental model of tumor invasion,” *Cancer Research*, vol. 66, pp. 1597–1604, 2006.
69. J. Langer, “Instabilities and pattern formation in crystal growth,” *Reviews of Modern Physics*, vol. 52, no. 1, pp. 1–30, 1980.
70. G. Cheng, J. Tse, R. Jain, and L. Munn, “Microenvironmental mechanical stress controls tumor spheroid size and morphology by suppressing proliferation and inducing apoptosis in cancer cells,” *PLoS ONE*, vol. 4, no. 2, p. e4632, 2009.
71. F. Montel, M. Delarue, J. Elgeti, L. Malaquin, M. Basan, T. Risler, B. Cabane, D. Vignjević, J. Prost, G. Cappello, and J. F. Joanny, “Stress clamp experiments on multicellular tumor spheroids,” *Physical Review Letters*, vol. 107, no. 18, p. 188102, 2011.
72. K. Alessandri, B. R. Sarangi, V. V. Gurchenkov, B. Sinha, T. R. Kieβling, L. Fetler, F. Rico, S. Scheuring, C. Lamaze, A. Simon, S. Geraldo, D. Vignjević, H. Doméjean, L. Rolland, A. Funfak, J. Bibette, N. Bremond, and P. Nassoy, “Cellular capsules as a tool for multicellular spheroid production and for investigating the mechanics of tumor progression in vitro,” *PNAS*, vol. 110, no. 37, pp. 14843–14848, 2013.
73. R. K. Jain, J. D. Martin, and T. Stylianopoulos, “The role of mechanical forces in tumor growth and therapy,” *Annual review of biomedical engineering*, vol. 16, pp. 321–346, 2014.
74. K. Kopanska, Y. Alcheikh, R. Staneva, D. Vignjevic, and T. Betz, “Tensile Forces Originating from Cancer Spheroids Facilitate Tumor Invasion,” *PLoS ONE*, vol. 11, no. 6, p. e0156442, 2016.
75. P. Provenzano, K. Eliceiri, J. Campbell, D. Inman, J. White, and P. Keely, “Collagen reorganization at the tumor-stromal interface facilitates local invasion,” *BMC Med*, vol. 4, p. 38, 2006.
76. L. Kaufman, C. Brangwynne, K. Kasza, E. Filippidi, V. Gordon, T. Deisboeck, and D. Weitz, “Glioma Expansion in Collagen I Matrices: Analyzing Collagen Concentration-Dependent Growth and Motility Patterns,” *Biophysical Journal*, vol. 89, p. 635650, 2005.
77. K. Wolf, M. Te Lindert, M. Krause, S. Alexander, J. Te Riet, A. Willis, R. Hoffman, C. Figdor, S. Weiss, and P. Friedl, “Physical limits of cell migration: Control by ECM space and nuclear deformation and tuning by proteolysis and traction force,” *The Journal of Cell Biology*, vol. 201, pp. 1069–1084, 2013.
78. A. Haeger, M. Krause, K. Wolf, and F. P., “Cell jamming: collective invasion of mesenchymal tumor cells imposed by tissue confinement,” *Biochimica et Biophysica Acta*, vol. 1840, no. 8, pp. 2386–95, 2014.
79. C. Giverso, A. Grillo, and L. Preziosi, “Influence of nuclear deformability on cell entry into cylindrical structures,” *Biomechanics and Modeling in Mechanobiology*, vol. 13, pp. 481–502, 2014.
80. A. Arduino and L. Preziosi, “A multiphase model of tumour segregation in situ by a heterogeneous extracellular matrix,” *International Journal of Non-Linear Mechanics*, vol. 75, pp. 22–30, 2015.
81. C. Giverso, A. Arduino, and L. Preziosi, “How Nucleus Mechanics and ECM Microstructure Influence the Invasion of Single Cells and Multicellular Aggregates,” [submitted], 2016.
82. G. Sciumé, R. Santagiuliana, M. Ferrari, P. Decuzzi, and B. Schrefler, “A tumor growth model with deformable ECM,” *Physical Biology*, vol. 11, no. 6,

- 932 p. 065004, 2014.
933 83. R. K. Jain, “Barriers to drug delivery in solid tu-
934 mours,” *Scientific American*, vol. 271, no. 1, pp. 58–
935 65, 1994.